Joint NOMA Transmission in Indoor Multi-cell VLC Networks

Virendra Singh Rajput, Ashok D. R., and A. Chockalingam
Department of ECE, Indian Institute of Science, Bangalore 560012

***Abstract*—In this paper, we consider downlink multiuser communication in indoor visible light communication (VLC) networks with multiple attocells using non-orthogonal multiple access (NOMA) transmission. We propose a joint NOMA transmission scheme, where the users in multi-cell overlapping regions are jointly served by all the corresponding VLC access points. For the proposed scheme, we consider efficient subcarrier allocation techniques, namely, area based subcarrier allocation and user based subcarrier allocation. Our performance results show that the proposed joint transmission scheme achieves significantly higher sum rates compared to the frequency reuse factor-2 (FR-2) NOMA scheme which uses independent transmission across multiple attocells. In particular, the area based subcarrier allocation scheme performs better than FR-2 NOMA for large number of users and the user based subcarrier allocation scheme performs better than FR-2 NOMA for any number of users.**

Index Terms *– Visible light communication, multi-cell VLC networks, NOMA, joint multi-cell transmission, subcarrier allocation.*

I. Introduction

Visible light communication has been receiving considerable attention recently for wireless communication in indoor environments [1]. This is because light emitting diode (LED) based light sources (luminaires/light fixtures) used for indoor lighting purposes can be simultaneously used for transmission of data as well through intensity modulation of the LEDs by the information bit stream. The intensity modulated signals are detected by photo diodes (PDs) at the receiver to recover the transmitted data. The narrow modulation bandwidth of the LEDs (due to slow rise/fall times) limit the achieved data rates in VLC systems. Multiple-input multiple-output (MIMO) techniques [2],[3] can increase the spectral efficiency in VLC systems. Spatial reuse of the available spectrum resources is another important approach to improve the spectral efficiency in wireless systems [4]. Indoor environments where the large number of luminaires are installed for lighting (e.g., airports, hospitals, factories) offer the possibility of exploiting the benefits of spatial reuse in indoor VLC networks. Each luminaire can act as a VLC access point (VAP) serving multiple users within the illuminated area (referred to as an optical attocell). A VLC network with multiple attocells can have regions where the illumination from two or more luminaires overlap. This leads to the issue of co-channel interference for users who reside in the overlapping regions (i.e., inter-cell interference). Inter-cell interference can be mitigated using suitable subcarrier allocation [5] and fractional frequency reuse approaches [6].

Recently, non-orthogonal multiple access (NOMA), a multiple access approach being considered in 5G to enhance system capacity and user experience [7], is getting increased attention for use in multiuser VLC networks [8]-[11]. In NOMA, signals of different users are superposed in the power domain to enable the users to share the same resources. While [8]-[10] consider NOMA in single cell VLC systems, [11]-[12] consider NOMA in multi-cell VLC systems. NOMA in multi-cell VLC has been introduced in [11], where a gain ratio power allocation (GRPA) scheme based on the users' channel gains is proposed. Transmit power allocation is done in such a way that users with smaller channel gains are allotted higher transmit powers. The sum rate performance of GRPA in a two-cell multiuser VLC system has been investigated in [11]. Subsequently, a theoretical framework to analyze the outage and sum rate performance of GRPA in a single cell multiuser VLC system has been reported in [9], where it has been shown that NOMA can achieve a higher sum rate compared to orthogonal multiple access (OMA). Also, pairing of users with more distinctive channel conditions can achieve better performance. In [8], NOMA has been shown to achieve superior performance compared to OFDMA in a VLC system with illumination constraints.

We note that the papers on multi-cell NOMA VLC networks reported in the literature so far have not considered *joint NOMA transmission* that can avoid the problem of inter-cell interference. This forms the key focus in this paper. Specifically, we propose a joint NOMA transmission scheme, where the users in multi-cell overlapping regions are jointly served by all the corresponding VLC access points. This scheme allocates powers to the users present in the multi-cell overlapping regions based on their effective channel gains. In the proposed scheme, multiple access across the overlapping and non-overlapping regions in a cell is provided by using different set of subcarriers to avoid inter-cell interference and multiple access for the users within a given region is provided using NOMA. We consider two subcarrier allocation techniques for the proposed scheme. In the first subcarrier allocation technique, subcarriers are allocated to the regions within a cell based on their percentage area. In the second subcarrier allocation technique, subcarriers are allocated to the regions within a cell based on the number of users present in them. Numerical results show that the proposed joint transmission scheme achieves significantly higher sum rates compared to those achieved by frequency reuse factor 2 (FR-2) NOMA scheme which uses independent transmission across multiple attocells.

II. System Model

A. Multi-cell VLC network

Consider the indoor VLC system consisting of multiple LED luminaires within a room as shown in Fig. 1, where each

This work was supported in part by the J. C. Bose National Fellowship, Department of Science and Technology, Government of India, and by Tata Elxsi Limited, Bengaluru 560048, India.

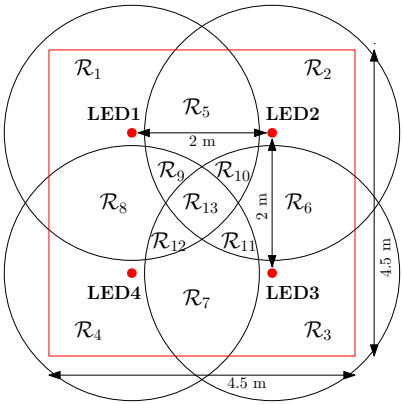

Fig. 1: Multi-cell (four-cell) VLC network. A '•' denotes an LED luminaire, the circle around it denotes its illumination region (attocell), and square in red denotes the boundaries of the room.

luminaire serves as a transmitter of an attocell. A '•' in Fig. 1 denotes an LED luminaire and the circle around it denotes its illumination region (cell). Observe that the illumination regions of these luminaires have overlaps among them as illustrated in Fig. 1. Regions $\mathcal{R}_i, i \in \{1,2,3,4\}$ denote the regions of no overlap, regions $\mathcal{R}_i, i \in \{5,6,7,8\}$ denote the regions of two-cell overlap, regions $\mathcal{R}_i, i \in \{9,10,11,12\}$ denote the regions of three-cell overlap, and $\mathcal{R}_{13}$ denotes the region of four-cell overlap. In this multi-cell network, each luminaire has 7 transmission regions (e.g., luminaire LED1 has transmission regions $\mathcal{R}_1$, $\mathcal{R}_5$, $\mathcal{R}_8$, $\mathcal{R}_9$, $\mathcal{R}_{10}$, $\mathcal{R}_{12}$, and $\mathcal{R}_{13}$). Among the 7 transmission regions of each luminaire (e.g., of luminaire LED1), only one region (e.g., $\mathcal{R}_1$) do not experience interference from any other luminaire, two regions (e.g., $\mathcal{R}_5$ and $\mathcal{R}_8$) experience interference from one luminaire, three regions (e.g., $\mathcal{R}_9$, $\mathcal{R}_{10}$, $\mathcal{R}_{12}$) experience interference from two luminaires, and only one region (e.g., $\mathcal{R}_{13}$) experiences interference from three luminaires.

B. Channel model

The line-of-sight (LOS) channel gain from a transmitter luminaire to a receiver PD is given by [13]

$$h = \frac{A}{d^2} L_r(\phi) F(\theta) C(\theta) \cos\theta, \tag{1}$$

where d is the distance between the transmitter luminaire and the receiver PD, A is the area of the PD, ϕ is the angle of emergence with respect to the normal at the transmitter, θ is the angle of incidence at the receiver with respect to its normal, Θ is the field of view (FOV) of the PD, $F(\theta)$ is the gain of optical filter, $L_r(\phi)$ represents the Lambertian radiation pattern of the luminaire, and $C(\theta)$ is the gain of optical concentrator. See Fig. 2 for definition of various parameters. The Lambertian radiation pattern of the luminaire is given by

$$L_r(\phi) = \frac{m+1}{2\pi} \cos^m \phi. \tag{2}$$

In the above equation, m represents the mode number, which is given by $m = -\ln 2 / \ln \cos \Phi_{\frac{1}{2}}$, where $\Phi_{\frac{1}{2}}$ is the half-

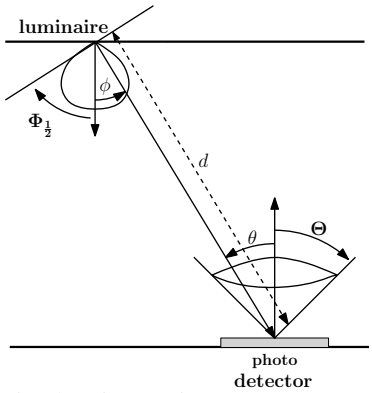

Fig. 2: Schematic showing various parameters which determine LOS path gain.

power semiangle of the transmitter luminaire. The gain of optical concentrator is expressed as

$$C(\theta) = \begin{cases} \frac{n^2}{\sin^2 \Theta}, & 0 \le \theta \le \Theta \\ 0, & \text{otherwise} \end{cases}, \tag{3}$$

where n denotes the refractive index.

III. Proposed Joint NOMA Transmission Scheme

In this section, we propose a joint NOMA transmission scheme for the multi-cell (four-cell) VLC network that is described in the Sec. II. We first discuss subcarrier allocation techniques in Sec. III-A. Then for a given subcarrier allocation, we discuss transmitter and receiver framework for the proposed scheme in Sec. III-B.

A. Subcarrier allocation

Each transmitter is provided with DCO-OFDM [14] modulator and each receiver is provided with DCO-OFDM demodulator as shown in the Fig. 3. The available bandwidth is divided among N subcarriers by DCO OFDM. Now, consider the luminaires and the regions as shown in Fig. 1. Each luminaire allocates different set of subcarriers to different regions within its attocell. Overlapping regions are assigned with same set of subcarriers by all the corresponding LEDs (e.g., LED1 and LED2 assign same set of subcarriers to the region $\mathcal{R}_5$). Let $\mathbb{N}$ denote the set of all subcarriers (note that $|\mathbb{N}| = N$), $\mathbb{N}_i$ denote the subset of $\mathbb{N}$ that is allocated to the region $\mathcal{R}_i$ by its corresponding LED/LEDs, and N_i denote the cardinality of the set $\mathbb{N}_i$, where $i \in \{1, 2, \cdots, 13\}$.

We consider two ways of choosing the subsets $\mathbb{N}_i$'s. The first way of choosing the subsets is based on the areas of the regions and the second way of choosing the subsets is based on the number of users residing in the regions. These techniques are described below.

1) Area based subcarrier allocation: A region having relatively large area has higher probability of having more number of users than a region having relatively small area. Therefore, in this allocation technique, the number of subcarriers allocated by a LED to a region is chosen in proportion to its area [6]. The

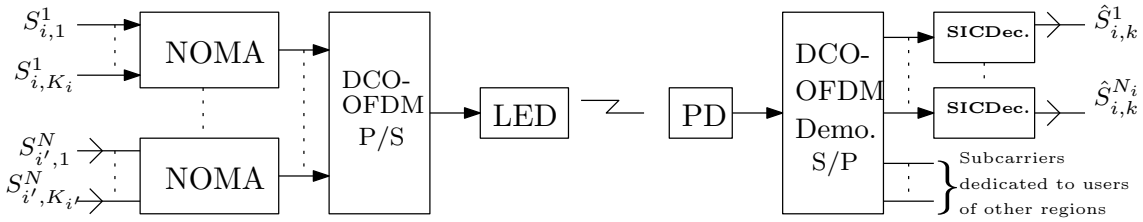

Fig. 3: Transmitter and receiver block diagram.

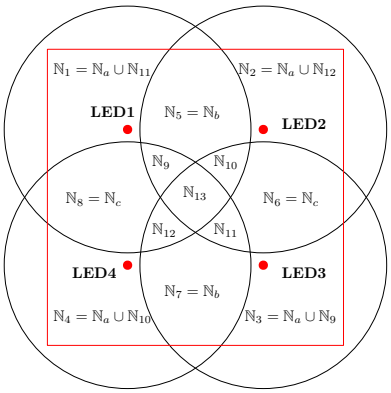

Fig. 4: Illustration showing the set of subcarriers allocated to different regions in the *area based subcarrier allocation*.

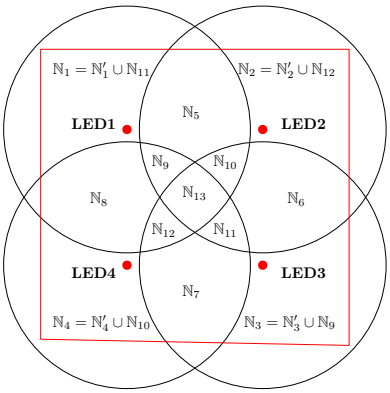

Fig. 5: Illustration showing the set of subcarriers allocated to different regions in the *user based subcarrier allocation*.

number of subcarriers allocated to the regions with multi-cell overlapping are given by

$$N_i = \left\lfloor \frac{A_i N}{A_{illum} + A'} \right\rfloor, \; i = 5, 6, \cdots, 13, \tag{4}$$

where A_i is the area of the region $\mathcal{R}_i$ (refer Fig. 1), A_{illum} is the area of illumination of an LED, and A' is the area of a region with three-cell overlap ($A' = A_9 = A_{10} = A_{11} = A_{12}$). Now, the number of subcarriers allocated to the non-overlapping regions are given by

$$N_i = N - \sum_{\substack{\mathcal{R}_l \in \mathbb{M}_i \\ l \neq i}} N_l, \; i = 1, 2, 3, 4, \tag{5}$$

where $\mathbb{M}_i$ represents the set of all the regions corresponding to the ith LED ($e.g., \mathbb{M}_1 = \{\mathcal{R}_1, \mathcal{R}_5, \mathcal{R}_8, \mathcal{R}_9, \mathcal{R}_{10}, \mathcal{R}_{12}, \mathcal{R}_{13}\}$). Due to symmetry, $(N_1 = N_2 = N_3 = N_4)$, $(N_5 = N_6 = N_7 = N_8)$, and $(N_9 = N_{10} = N_{11} = N_{12})$. The subsets $\mathbb{N}_i$'s with the cardinalities N_i's calculated based on (4) and (5) are chosen as shown in the Fig. 4, where $\mathbb{N}_a$, $\mathbb{N}_b$, $\mathbb{N}_c$, $\mathbb{N}_9$, $\mathbb{N}_{10}$, $\mathbb{N}_{11}$, $\mathbb{N}_{12}$, and $\mathbb{N}_{13}$ are pairwise disjoint and exhaustive subsets of $\mathbb{N}$. With this configuration, it is easy to verify that the subsets allocated to the regions in any given attocell are pairwise disjoint and exhaustive.

2) User based subcarrier allocation: In this proposed technique, the number of subcarriers allocated to a region by a transmitter is chosen based on the number of users residing in it. Let K_i represent the number of users residing in the region $\mathcal{R}_i$, and Q_j denote the number of users in the attocell corresponding to the jth LED. Also, consider $Q'_1 = Q_1 + K_{11}$, $Q'_2 = Q_2 + K_{12}$, $Q'_3 = Q_3 + K_9$, and $Q'_4 = Q_4 + K_{10}$. Now, the number of subcarriers allocated to the regions are obtained as follows.

1) For the regions having two or more cell overlap the number of subcarriers allocated by all the corresponding LEDs are given by

$$N_i = \left\lfloor \frac{K_i N}{\max_{j \in \mathbb{J}_i} \{Q'_j\}} \right\rfloor, \; i = 5, 6, \cdots, 13, \tag{6}$$

where $\mathbb{J}_i$ denotes the set of all LEDs that transmit to the region $\mathcal{R}_i$.

2) Given the number of subcarriers allocated to the overlapping regions, the number of subcarriers allocated to the non-overlapping regions are obtained by using (5).

Now, the subsets $\mathbb{N}_i$'s with the cardinalities N_i's calculated based on (5) and (6) are chosen as shown in the Fig. 5. The subsets of subcarriers allocated by any luminaire to the corresponding regions are pairwise disjoint and exhaustive (e.g., $\mathbb{N}_1$, $\mathbb{N}_5$, $\mathbb{N}_8$, $\mathbb{N}_9$, $\mathbb{N}_{10}$, $\mathbb{N}_{12}$, and $\mathbb{N}_{13}$ are pairwise disjoint and exhaustive subsets of $\mathbb{N}$).

Note that in area based subcarrier allocation technique, allocation of the subcarriers is independent of the total number of users and also the locations of the users present in the multi-cell VLC network. Therefore, subcarrier allocation has to be done only once, which makes area based subcarrier allocation

simpler compared to user based subcarrier allocation. However, user based subcarrier allocation can provide better performance by adapting to the changes in either the total number of users or locations of the users.

B. Joint NOMA transmitter and receiver framework

In the proposed scheme, multiple access across the regions is provided by allocating different set of subcarriers and multiple access to the users within any given region is provided using NOMA. For all the users in a given region, an independent NOMA symbol is broadcast by the corresponding luminaires on each of the allocated subcarrier. The NOMA symbol transmitted by the jth LED on a subcarrier $n \in N_i$ which is intended for the users in the region $\mathcal{R}_i$ is given by

$$X_i^{j,n} = \sum_{k \in \mathbb{K}_i} S_{i,k}^{j,n} \sqrt{P_{i,k}^{j,n}}, \tag{7}$$

where $\mathbb{K}_i = \{1, 2, \cdots, K_i\}$, $S_{i,k}^{j,n}$ represents the modulation symbol transmitted by the jth LED on the nth subcarrier intended to the kth user of the region $\mathcal{R}_i$, $P_{i,k}^{j,n}$ represents the power allocated by the jth LED for the nth subcarrier to the kth user of the region $\mathcal{R}_i$.

In the proposed scheme, for any given user k in a multi-cell overlap region $\mathcal{R}_i$, on a given subcarrier n, same modulation symbol is transmitted by all the corresponding LEDs with same power, i.e.,

$$S_{i,k}^{j,n} = S_{i,k}^{n}, \ \forall j \in \mathbb{J}_i, \ \forall k \in \mathbb{K}_i, \tag{8}$$

$$P_{i,k}^{j,n} = P_{i,k}^{n}, \ \forall j \in \mathbb{J}_i, \ \forall k \in \mathbb{K}_i. \tag{9}$$

The procedure to obtain the $P_{i,k}^n$'s is described in Sec. III-C.

At each transmitter, the NOMA symbols are transmitted using DCO-OFDM block which performs Hermitian symmetry, IDFT, and DC biasing operations [14]. Each receiver performs DC bias compensation, DFT, and inverse of Hermitian symmetry operations to obtain the NOMA symbols. The NOMA symbol received on the subcarrier $n \in \mathbb{N}_i$ by the kth user in the region $\mathcal{R}_i$ is given by

$$\begin{aligned} Y_{i,k}^n &= a \sum_{j \in \mathbb{J}_i} h_{i,k}^{j,n} X_i^{j,n} + N_{i,k}^n \\ &= a \sum_{j \in \mathbb{J}_i} h_{i,k}^{j,n} \sum_{k' \in \mathbb{K}_i} S_{i,k'}^{j,n} \sqrt{P_{i,k'}^{j,n}} + N_{i,k}^n, \ k \in \mathbb{K}_i, \end{aligned} \tag{10}$$

where $h_{i,k}^{j,n}$ denotes the channel gain from the jth LED to the kth user of the region $\mathcal{R}_i$ for the nth subcarrier, a denotes the responsivity of PD (in Ampere/Watt), $N_{i,k}^n \sim \mathcal{N}(0, \sigma^2)$ denotes the noise corresponding to the kth user of region $\mathcal{R}_i$ for the nth subcarrier.

Using (8) and (9), (11) can be simplified as

$$Y_{i,k}^n = a \tilde{h}_{i,k}^n \Big(S_{i,k}^n \sqrt{P_{i,k}^n} + \sum_{\substack{k' \in \mathbb{K}_i \\ k' \neq k}} S_{i,k'}^n \sqrt{P_{i,k'}^n} \Big) + N_{i,k}^n, \tag{11}$$

Algorithm 1 SIC decoding for the kth user on nth subcarrier

1: **Inputs**: k, $Y_{i,k}^n, \mathbb{K}_i$, $P_{i,1}^n, P_{i,2}^n, \cdots, P_{i,K_i}^n$, $\tilde{h}_{i,1}^n, \tilde{h}_{i,2}^n, \cdots, \tilde{h}_{i,K_i}^n$, modulation alphabet ($\mathbb{A}$).
2: **Initialize**: $\tilde{Y} = Y_{i,k}^n$; set $\mathbb{S} = \mathbb{K}_i$.
3: **do**
4: $\quad l = \text{argmax}_{k' \in \mathbb{S}} \ P_{i,k'}^n$
5: $\quad \hat{S}_{i,l}^n = \text{argmin}_{S \in \mathbb{A}} \ \|\tilde{Y} - a\tilde{h}_{i,l}^n S \sqrt{P_{i,l}^n}\|$
6: $\quad \tilde{Y} = \tilde{Y} - a\tilde{h}_{i,l}^n \hat{S}_{i,l}^n \sqrt{P_{i,l}^n}$
7: $\quad \mathbb{S} = \mathbb{S} \backslash \{l\}$
8: **while**$(l \neq k)$
9: **Output**: $\hat{S}_{i,k}^n$

where $\tilde{h}_{i,k}^n$ is sum of the channel gains (i.e., effective channel gain) to the kth user of the region $\mathcal{R}_i$ from all the corresponding LEDs, i.e.,

$$\tilde{h}_{i,k}^n = \sum_{j \in \mathbb{J}_i} h_{i,k}^{j,n}, \ k \in \mathbb{K}_i. \tag{12}$$

Each receiver uses successive interference cancellation (SIC) [15] to decode their modulation symbols. The SIC decoding procedure for user $k \in \mathbb{K}_i$ is presented in Algorithm 1.

C. Transmit power allocation

Without loss of generality, let us assume $h_{i,1}^{j,n} \leq h_{i,2}^{j,n} \leq \cdots \leq h_{i,K_i}^{j,n}$. For the users in a non-overlapping region $\mathcal{R}_i, i \in \{1, 2, 3, 4\}$, on a given subcarrier n, the allocated powers by the corresponding LED are iteratively obtained using GRPA technique [11] as

$$P_{i,k}^n = \left(\frac{h_{i,1}^{j,n}}{h_{i,k}^{j,n}} \right)^k P_{i,k-1}^n, \ k = 1, 2, \cdots, K_i, \ j = i. \tag{13}$$

For the users in a multi-cell overlapping region $\mathcal{R}_i, i \in \{5, 6, \cdots, 13\}$, on a given subcarrier n, the power allocated by all the corresponding LEDs is given by

$$P_{i,k}^n = \left(\frac{\tilde{h}_{i,1}^n}{\tilde{h}_{i,k}^n} \right)^k P_{i,k-1}^n, \ k = 1, 2, \cdots, K_i. \tag{14}$$

Again, without loss of generality, in the above equation $\tilde{h}_{i,1}^n \leq \tilde{h}_{i,2}^n \leq \cdots \leq \tilde{h}_{i,k_i}^n$ is assumed.

D. SINR and achievable rate

With SIC decoding, the received SINR for the kth user of region $\mathcal{R}_i$ on the nth subcarrier assuming $P_{i,1}^n \geq P_{i,2}^n \geq \cdots \geq P_{i,K_i}^n$ is given by

$$\gamma_{i,k}^n = \frac{a^2 (\tilde{h}_{i,k}^n)^2 P_{i,k}^n}{a^2 \Big(\sum\limits_{r=k+1}^{K_i} (\tilde{h}_{i,r}^n)^2 P_{i,r}^n + \xi \sum\limits_{\hat{r}=1}^{k-1} (\tilde{h}_{i,\hat{r}}^n)^2 P_{i,\hat{r}}^n \Big) + \sigma^2}, \tag{15}$$

where ξ denotes residual factor which accounts for interference due to incorrectly decoded symbols corresponding to users

$1, 2, \cdots, k-1$ [16]. The achievable rate for the kth user of region R_i on the nth subcarrier is given by

$$\eta_{i,k}^{n} = \frac{B}{2N} \log_2 \left(1 + \gamma_{i,k}^{n}\right), \tag{16}$$

where B denotes the modulation bandwidth of the LEDs.

IV. Results and Discussions

In this section, we compare the sum rate performance of the proposed joint NOMA scheme with that of FR-2 NOMA [12] scheme for the LOS VLC channel. The parameters considered for the simulations are given in Table I. Note that the sum rate performance in Figs. 6, 7, and 8 are obtained by averaging over large number of user locations that are obtained using uniform random distribution.

In Fig. 6, we present the sum rate performance of the proposed scheme and FR-2 NOMA scheme as a function of number of users distributed across the room for ξ= 0.01 and 0.1. It can be observed that the proposed scheme with the user based subcarrier allocation outperforms FR-2 NOMA scheme. The proposed scheme with the area based subcarrier allocation performs better than FR-2 NOMA for large number of users. For example, the gain in the sum rate for the proposed scheme with the area based subcarrier allocation as compared to FR-2 NOMA for 12 users is about 8 Mbps and gain in the sum rate for the proposed scheme with the user based subcarrier allocation for 12 users is about 25 Mbps. The reasons for the gain in the sum rate performance of the proposed scheme are as follows. Each LED in FR-2 NOMA utilizes only half of the available bandwidth, whereas in the proposed scheme the available bandwidth is completely utilized by all the LEDs due to efficient subcarrier allocation. Also, in the proposed scheme, the users in the overlapping regions receive data from multiple LEDs, thereby increasing their received SINR. In the area based subcarrier allocation, subcarriers will also be allocated to the regions having no users. There will be some regions with no users when the number of users is less. Therefore, some subcarriers will not be used in the case of the area based allocation when the number of users is less. Hence,

Parameters	Notation	Value
Transmit signal power	P_{ele}	1 mW
User height	d_r	0.85 m
Transmitter LED height	d_t	3 m
Room dimension	-	4.5 m×4.5 m×3 m
Half power semi-angle	$\Phi_{\frac{1}{2}}$	60^o
Signal bandwidth	B	20 MHz
Power spectral density of noise	N_o	$10^{-21} W/Hz$
PD field of view	Θ	38^o
Area of PD	A	$10^{-4}\ m^2$
Responsivity of PD	α	0.3 A/W
Gain of optical filter	$F(\theta)$	1
Refractive index	n	1.5

TABLE I: Simulation parameters.

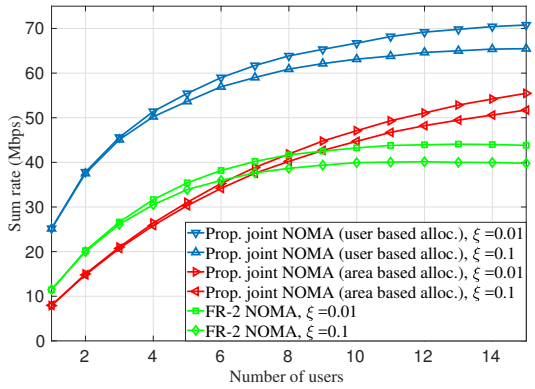

Fig. 6: Sum rate performance of the proposed scheme and FR-2 NOMA scheme as a function of number of users distributed in whole room area.

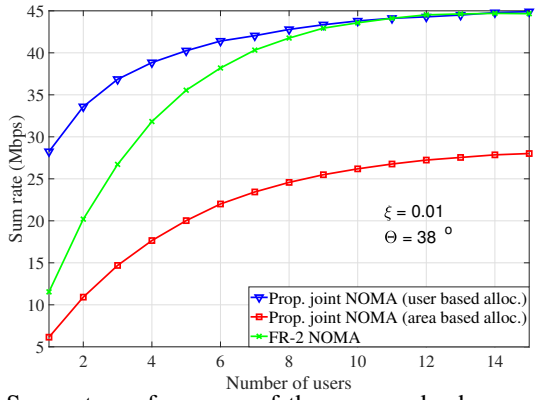

Fig. 7: Sum rate performance of the proposed scheme and FR-2 NOMA scheme as a function of number of users distributed only in overlapping regions.

the performance of the proposed scheme with the area based allocation is poor for less number of users.

Next, in Figs. 7 and 8, we compare the sum rate performance of the proposed scheme with FR-2 NOMA scheme as a function of number of users for the cases in which the users are distributed only in overlapping regions and only in non-overlapping regions, respectively. For the case in which users are distributed only in overlapping regions, it can be observed that the proposed scheme with user based subcarrier allocation performs better than FR-2 NOMA for small number of users (for less than 9 users) and the performance of both the schemes are nearly the same for large number of users. The proposed scheme with area based subcarrier allocation performs worse than FR-2 NOMA. For the case in which users are distributed only in non-overlapping regions, we can observe that the proposed scheme with user based subcarrier allocation performs better than FR-2 NOMA almost by a factor of 2. This is because in the proposed scheme with user based subcarrier allocation, all the subcarriers will be allocated to non-overlapping regions by the LEDs which makes the bandwidth available to the users twice than that in FR-2 NOMA. Again, the

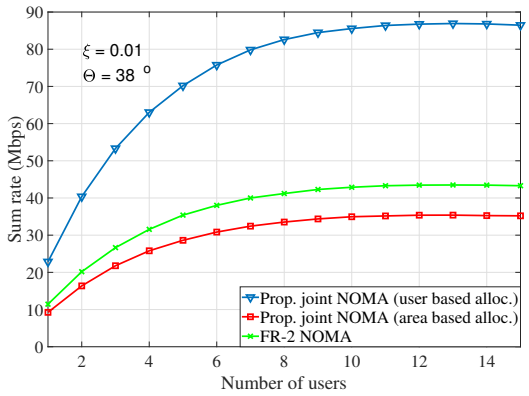

Fig. 8: Sum rate performance of the proposed scheme and FR-2 NOMA scheme as a function of number of users distributed only in non-overlapping regions.

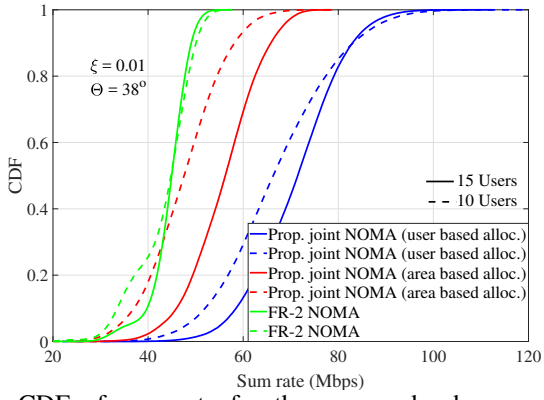

Fig. 9: CDF of sum rate for the proposed scheme and FR-2 NOMA scheme.

proposed scheme with area based subcarrier allocation performs worse than FR-2 NOMA. This happens because the subcarrier allocated to overlapping regions are left unused.

Finally, in Fig. 9, we present the cumulative distribution function (CDF) of the sum rate for the proposed scheme and FR-2 NOMA scheme for 10 and 15 users with $\xi = 0.01$ in Fig. 9. We can observe that for 10 users, the sum rate achieved by FR-2 NOMA is in the range of 20-50 Mbps, the sum rate achieved by the proposed scheme with the area based allocation is in the range of 30-75 Mbps, and the sum rate achieved by the proposed scheme with the user based allocation is in the range of 35-95 Mbps. In case of 15 users, for all the three schemes, ranges of the sum rate are nearly the same as for the case of 10 users, but the medians are increased by approximately 5 Mbps for the proposed scheme with user based allocation and 10 Mbps for the proposed scheme with area based allocation. But there is no significant change in the median for FR-2 NOMA scheme as we increase the number of users from 10 to 15.

V. Conclusions

We studied multiuser communication in indoor VLC networks with multiple attocells on the downlink using NOMA transmission. We proposed a joint NOMA transmission scheme in which the users in multi-cell overlapping regions are jointly served by all the corresponding luminaires. For the proposed scheme, we considered two subcarrier allocation techniques, namely, area based subcarrier allocation and user based subcarrier allocation. We compared the performance of the proposed scheme with that of the FR-2 NOMA scheme known in the literature. Our results showed that the proposed scheme with area based subcarrier allocation performs better than the FR-2 NOMA for large number of users and the proposed scheme with user based subcarrier allocation performs better than FR-2 NOMA for any number of users. Further, joint NOMA transmission scheme for multi-cell VLC networks with illumination constraints can be taken up as an interesting topic for further research.

References

[1] P. H. Pathak, X. Feng, P. Hu, and P. Mohapatra, "Visible light communication, networking, and sensing: a survey, potential and challenges," *IEEE Commun. Surveys & Tutorials*, vol. 17, no. 4, pp. 2047-2077, 4th quarter 2015.

[2] T. Fath and H. Haas, "Performance comparison of MIMO techniques for optical wireless communications in indoor environments," *IEEE Trans. Commun.*, vol. 61, no. 2, pp. 733-742, Feb. 2013.

[3] A. K. Gupta and A. Chockalingam, "Performance of MIMO modulation schemes with imaging receivers in visible light communication," *J. Lightw. Technol.*, vol. 36, no. 10, pp. 1912-1927, May 2018.

[4] M. Alouini and A. Goldsmith, "Area spectral efficiency of cellular mobile radio systems," *IEEE Trans. Veh. Technol.*, vol. 48, no. 4, pp. 1047-1066, Jul. 1999.

[5] H. Kim, D. Kim, S. Yang, Y. Son, and S. Han, "Mitigation of inter-cell interference utilizing carrier allocation in visible light communication system," *IEEE Commun. Lett.*, vol. 16, no. 4, pp. 526-529, Apr. 2012.

[6] C. Chen, D. Tsonev, and H. Haas, "Fractional frequency reuse in DCO-OFDM-based optical attocell networks," *J. Lightw. Technol.*, vol. 33, no. 19, pp. 3986-4000, Oct. 1, 2015.

[7] S. M. R. Islam et al., "Power-domain non-orthogonal multiple access (NOMA) in 5G systems: potentials and challenges," *IEEE Commun. Surveys & Tutorials*, vol. 19, no. 2, pp. 721-742, Oct. 2016.

[8] R. C. Kizilirmak, C. R. Rowell, and M. Uysal, "Non-orthogonal multiple access (NOMA) for indoor visible light communications," in *Proc. Int. Workshop Opt. Wireless Commun.*, Sep. 2015, pp. 98-101.

[9] L. Yin, O. Wasiu, X. Wu, and H. Haas, "Performance evaluation of non-orthogonal multiple access in visible light communication," *IEEE Trans. Commun.*, vol. 64, no. 12, pp. 5162-5175, Dec. 2016.

[10] H. Marshoud et al., "On the performance of visible light communication systems with non-orthogonal multiple access," *IEEE Trans. Wireless Commun.*, vol. 16, no. 10, pp. 6350-6364, Oct. 2017.

[11] H. Marshoud, V. M. Kapinas, G. K. Karagiannidis, and S. Muhaidat, "Non-orthogonal multiple access for visible light communications," *IEEE Photon. Technol. Lett.*, vol. 28, no. 1, pp. 51-54, Jan. 1, 2016.

[12] X. Zhang, Q. Gao, C. Gong, and Z. Xu, "User grouping and power allocation for NOMA visible light communication multi-cell networks," *IEEE Commun. Lett.*, vol. 21, no. 4, pp. 777-780, Apr. 2017.

[13] J. M. Kahn and J. R. Barry, "Wireless infrared communications," *Proceedings of the IEEE*, vol. 85, no. 2, pp. 265-298, Feb. 1997.

[14] O. Gonzalez et al., "OFDM over indoor wireless optical channel," *Proc. IEE Optoelectron.*, vol. 152, no. 4, pp. 199-204, Aug. 2005.

[15] Z. Ding, Z. Yang, P. Fan, and H. V. Poor, "On the performance of non-orthogonal multiple access in 5G systems with randomly deployed users," *IEEE signal process. Lett.*, vol. 21, no. 12, pp. 1501-1505, Dec. 2014.

[16] J. G. Andrews and T. H. Meng, "Optimum power control for successive interference cancellation with imperfect channel estimation," *IEEE Trans. Wireless Commun.*, vol. 2, no. 2, pp. 375-383, Mar. 2003.